Vivien.

EUROPEAN ORGANIZATION FOR NUCLEAR RESEARCH
ORGANISATION EUROPEENNE POUR LA RECHERCHE NUCLEAIRE

CERN - PS DIVISION

PS/ CA/ Note97-11

MAGNETIC MEASUREMENTS ON
BOOSTER TRANFER SEPTUM MAGNET VERTICAL 20

J. Borburgh

Geneva, Switzerland
24 April 1997

1. Introduction

Before installation in the booster transfer line complex it was necessary to test the magnet SMV 20 and its reserve at various currents corresponding to the various beam energies required. Tests were carried out to perform magnetic measurements and compare with the calculated design values at different current levels. The results of these tests are tabulated in this report.

Figure 1 shows an equivalent circuit diagram and the positions where induction measurements were made are marked with B. In figure 2 the positions of the measurement coils are indicated where the different magnetic measurements were taken.

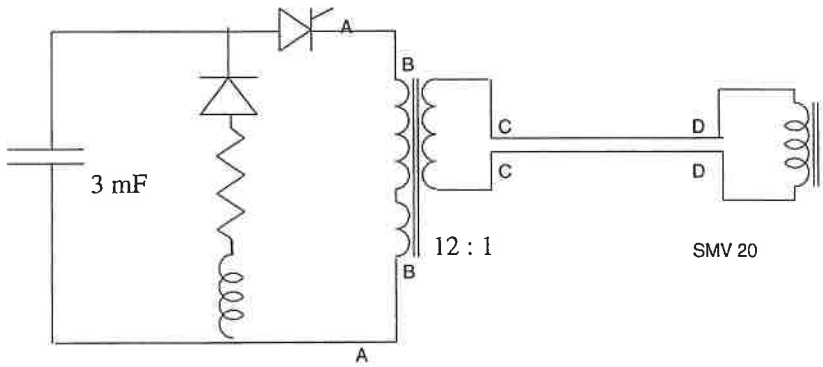

Figure 1: the circuit diagram

The measurement equipment used for the inductance measurements and the magnet measurements was:

Impedance meter	Philips Fluke PM 6304
Current Transformer	Pearson Model 1423 (1 V/kA)
Digitiser	Tektronix 7612D
Data handling	486 p.c. with Labview
Scope	H.P. Model 54601 A

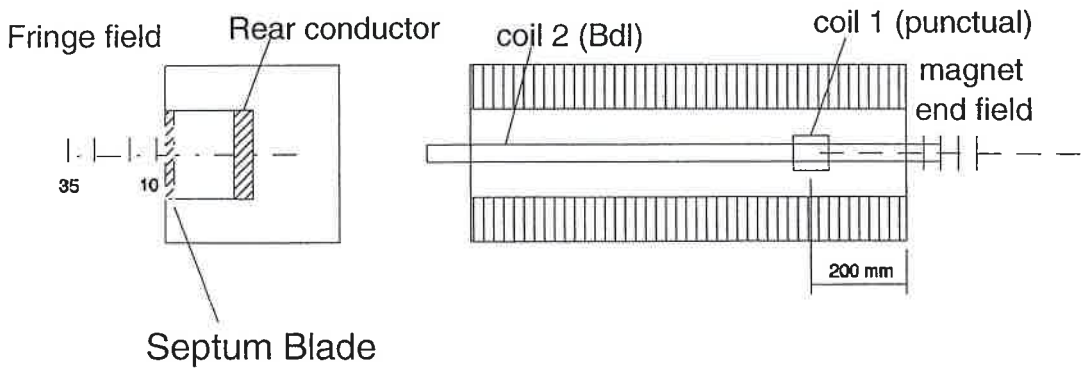

Figure 2: magnetic measurement positions

2. Inductance measurements

The inductance of the magnet itself was calculated at 2.27 μH for a quasi dc situation. Using an impedance meter the individual values for the inductance of the discharge circuit were measured at point B in Figure 1. By bridging the circuit at point D the inductance as seen by the primary of the power supply (point B, figure 1) can be determined. In table 1 the results are reproduced.

Table 1 : inductance measurements on magnet SMV20.2

Measurement frequency	100Hz	1 kHz
Inductance with:		
short circuit @ D (μH)	55.0	51.9
no short circuit (μH)	388.6	372.2
Derived magnet inductance (μH)	**2.3**	**2.2**

The magnet SMV20.1 is build exactly the same, so it was no surprise that the inductance measurement was the same. The values measured on SMV20.1 are very close to the values calculated. Since the old magnet used to be was a twelve turn DC magnet, these new magnets have a much lower inductance.

3. Current Characteristics

The septum magnets were connected to the power supply as shown in figure 1 of this report. The capacitor bank was 3 mF. The current wave form was measured for magnet SMV20.2. Three characteristic quantities can be defined:

-I_{top}, the top value of the current
-T_{top}, time from start until I_{top} occurs
-$T_{\frac{1}{2}\omega}$, the length of the half sine

For I_{top} = 25.2 kA these quantities are tabulated in table 2, and the current wave form itself is shown in figure 3.

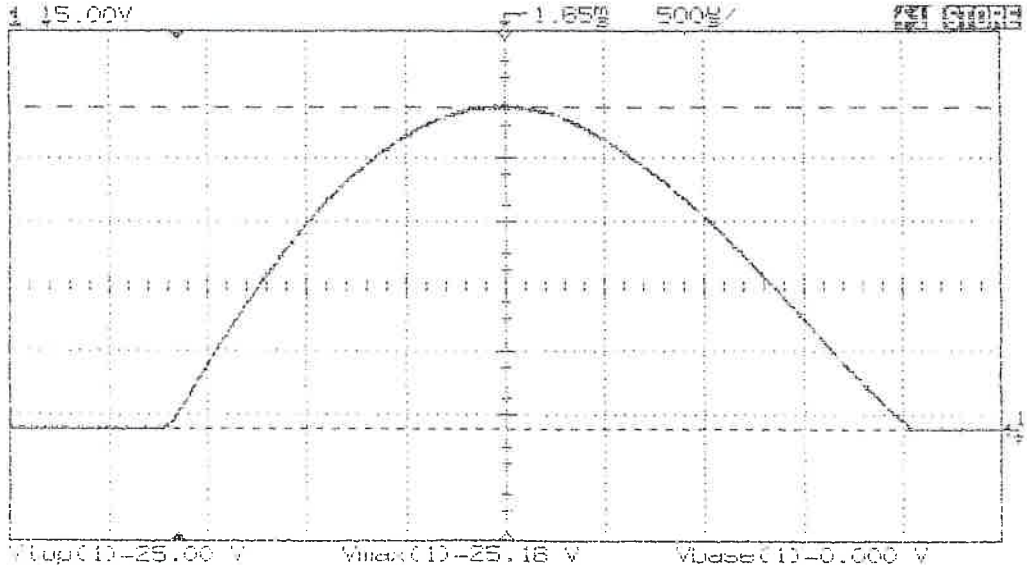

Figure 3: current wave form of SMV 20.2 at 25.2 kA

Table 2: T_{top} and $T_{\P/\omega}$ for different currents of the magnet

I_{top} (kA)	25.2 kA
$T_{\P/\omega}$ (ms)	3.75 ms
T_{top} (ms)	1.70 ms

4. Magnetic measurements

Using the power supply described previously with a pulse repetition rate of approximately 4.5 seconds a series of measurements were recorded in order to determine the magnetic field in the gap, the fringe field, close to the septum, and the end. The field in the gap was measured to determine the actual punctual values and also the integrated field (Bdl) from which we can calculate the equivalent magnetic length of the magnet. Three measuring coils were used and their characteristics are given below.

a. For punctual field values,

Coil 1; surface area = 0.03693m^2 ; (∅ = 5 mm)^2

b. For Bdl measurements,

Coil 2; specific surface=0.05763 m^2/m; (Surface area = 0.0750m^2, length 1.30 m)
Coil 3; specific surface = 0.05808 m^2/m; (Surface area = 0.0755m^2, length 1.30 m)

With the small measuring coil (coil 1) the field was measured in the middle of the gap at one quarter of the length of the septum. With the program 'fringe field measurement' running under Labview, the fields were measured. This program is derived from the program 'B measurementv311' described in note PS/PA 95-13.

All results of the magnetic measurements are tabulated and illustrated in Appendix I.

4.1 Measurements inside the magnet gap

In this paragraph diagrams are shown of the field in the gap, measured with coil 1, and the integrated field through the gap measured over more than the full length of the magnet to obtain the equivalent length of the magnet. The results of the measurements for both magnets SMV20 are shown in figures 4a and 4b.

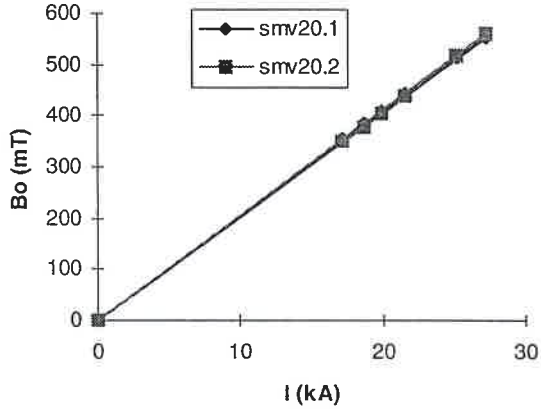

Figure 4a: B_0 measurement in the gap

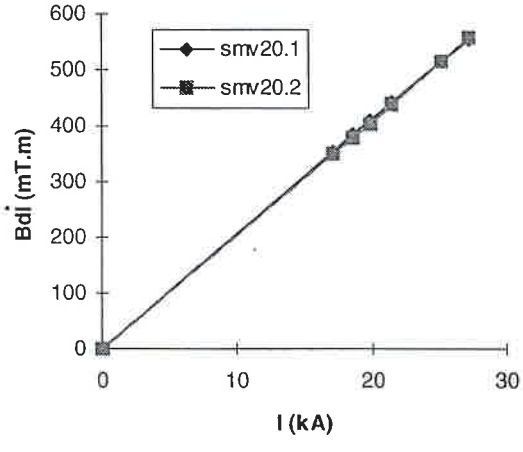

Figure 4b: Bdl measurements in the gap

What can be noticed is, that no measurable saturation occurs, even for very large currents.

The equivalent length (L_{equiv}) of both magnets, as derived from the magnetic measurements is tabulated in table 3. This length is calculated by dividing the integrated field by the corresponding field strength. The table show little variation in L_{eq} for each magnet, what indicates there is no saturation. However some difference can be noticed between the two magnets. Since they are physically identical it is suspected that the coil1 used for the measurements of SMV 20.2 was not correctly parallel to the gap field.

The calculated equivalent magnetic length with the finite element program Tosca is 1003 mm and the measured length is approximately 0.5 % longer than was measured. The difference may be explained by the lack of accuracy of the 3 dimensional Tosca model which could not to be meshed dense enough, to prevent memory overflow of the computer.

Take this one

This is really installed

Table 3: the equivalent magnetic length as function of the current

I (kA)	Leq (mm) SMV 20.1	Leq (mm) SMV 20.2
17.2	998	995
18.6	999	997
19.9	998	995
21.6	995	995
25.1	999	996
27.2	1000	993

4.2 Measurement of the fringe field next to the septum

Measurements were carried out to determine the magnitude of the integrated fringe field parallel and close to the septum blade in order to assess the effect of a pulsing magnet on the orbiting beam. The results were taken at several separate distances from the septum and are graphically shown in figure 5.

The fringe filed for both magnets falls below $1/1000^{th}$ of the gap field at 55 mm from the septum blade. This is good enough for a magnet in a transfer line to not adversely affect the 'orbiting' beam.

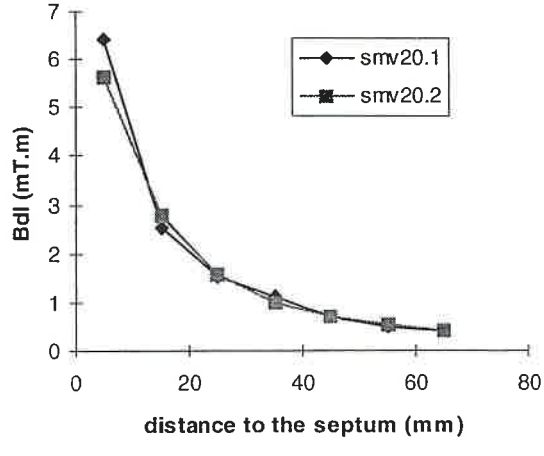

Figure 5: Integrated fringe field measurements for I = 25.2 kA

4.3 Measurement of the leakage field at the end of the magnet

The field was measured at several positions in front of the middle of the magnet gap to determine the magnitude of the end field. The measurements have been taken for two different currents. The results are illustrated in figure 6 together with the calculation of the end field with Tosca.

This field contributes to the magnetic length of the magnet. What can be seen in figure 6 is that the end fields drop very rapidly, as can be expected. But the measurements of the two different magnets seem not to be consistent. The measurements on SMV 20.1 are not dropping very rapidly and are also high in absolute value. Since the magnetic length as measured for this magnet is close to the calculated one and close to the one measured on SMV 20.2, the explanation must be an error in the measurement equipment.

The difference between the calculated field with a 3 dimensional Tosca model and the measurements on SMV 20.2 may be related with the precision of positioning of the measurement coil, since the end field drops rapidly.

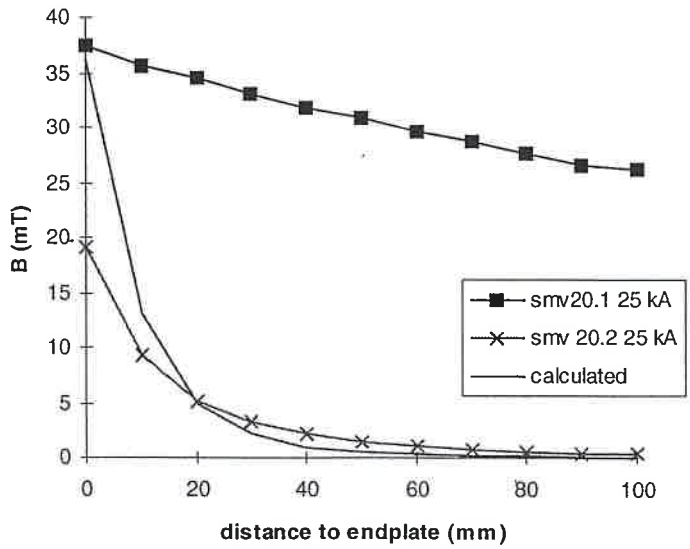

Figure 6: End field decay as measured from the outside of the endplate

5. Conclusions

The inductance measurements have shown that the measured values for the new magnets are within 5% of the calculated ones.

The current wave forms are measured and are as can be expected.

The magnetic equivalent length of the magnets is close to the calculations. The physical size of the magnet prevented an accurate calculation and explains the 0.5% difference between the calculation and the measurement.

Leakage fields at the ends of the new magnet are as expected. The calculated end field decay is close to what is measured on the septum SMV 20.2. When measuring the end field of SMV 20.1 the end field does not decay as quickly as supposed to. But since the magnet equivalent length of this magnet is very close to the calculations, it is assumed that an error has occurred during the end field measurements. The stray field next to the septum blade of the new magnets is low, lower then 1% of the gap field at 10 mm from the septum, and lower then 1/1000 at 50 mm distance from the septum.

Appendix I : The measurements

BTSMV 20.1

impédance (vu depuis le primaire du transfo)
L=388.3 μH (200 Hz)
R=0.0306 ohm (200 Hz)

Débit d'eau à 12 bar
Q = 3.8 l/min.

BTSMV 20.2

impédance (vu depuis le primaire du transfo)
L= 388.6 μH (100 Hz)
R=0.022 ohm (100 Hz)

Impédance stripline jusqu'à (point D)
L = 55 μH (100 Hz)

Débit d'eau à 12 bar
Q = xxxxx l/min.

SMV20.1

date test: 12/12/96

coil 1 dia. 5 mm; 0.037 m2 (Bo)

coil 2 l=1300 mm 0.058 m2/m (Bdl) 0.0750 m2

I (A)	coil1 Vdt	mT	coil2 Vdt	mTm	Leq mm	remarks
17172	1.314E-02	355.9	2.050E-02	355.3	0.998	angle 73.2 mrad with protons at 0.8 GeV
18600	1.420E-02	384.5	2.216E-02	384.1	0.999	angle 79.3 mrad with protons at 0.8 GeV
19900	1.514E-02	410.1	2.360E-02	409.3	0.998	angle 73.2 mrad with protons at 1.0GeV
21560	1.642E-02	444.5	2.550E-02	442.2	0.995	angle 79.3 mrad with protons at 1.0GeV
25131	1.901E-02	514.8	2.978E-02	514.1	0.999	angle 73.2 mrad with protons at 1.4GeV
27226	2.044E-02	553.5	3.195E-02	553.9	1.001	angle 79.3 mrad with protons at 1.4GeV

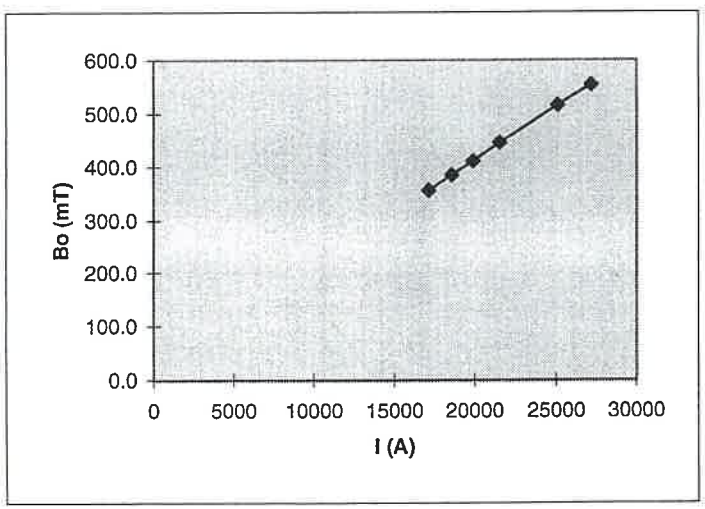

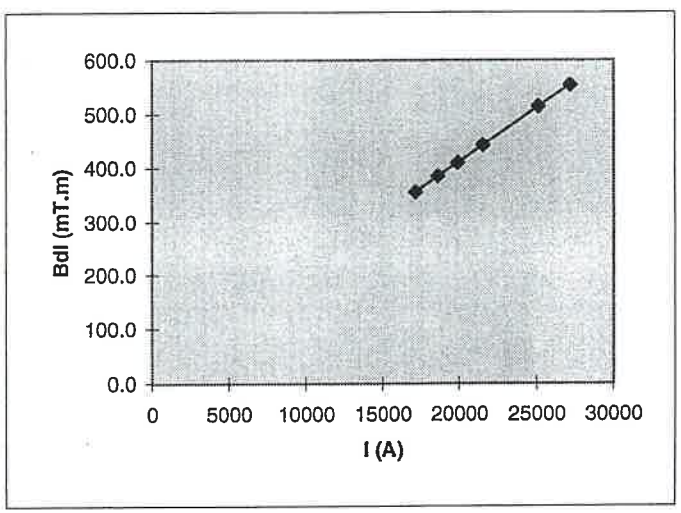

Fringefield SMV 20.1

date test: 12/12/96

coil 2 l=1300 mm 0.05769 m2/m

coil 3 l=1300 mm 0.05808 m2/m

distance to septum (mm)	Vdt (V.s) 1.0 GeV, 20 kA	Bdl (mT.m)	Vdt (V.s) 1.4 GeV, 25.16 kA	Bdl (mT.m)	
5	2.19E-04	4.288	3.72E-04	6.4	coil3
15	1.18E-04	2.05	1.46E-04	2.528	coil2
25	6.57E-05	1.139	8.85E-05	1.533	coil2
35	3.94E-05	0.6823	6.56E-05	1.136	coil2
45	2.84E-05	0.4915	4.09E-05	0.709	coil2
55	2.24E-05	0.3878	2.91E-05	0.504	coil2
65	1.84E-05	0.318	2.36E-05	0.4093	coil2

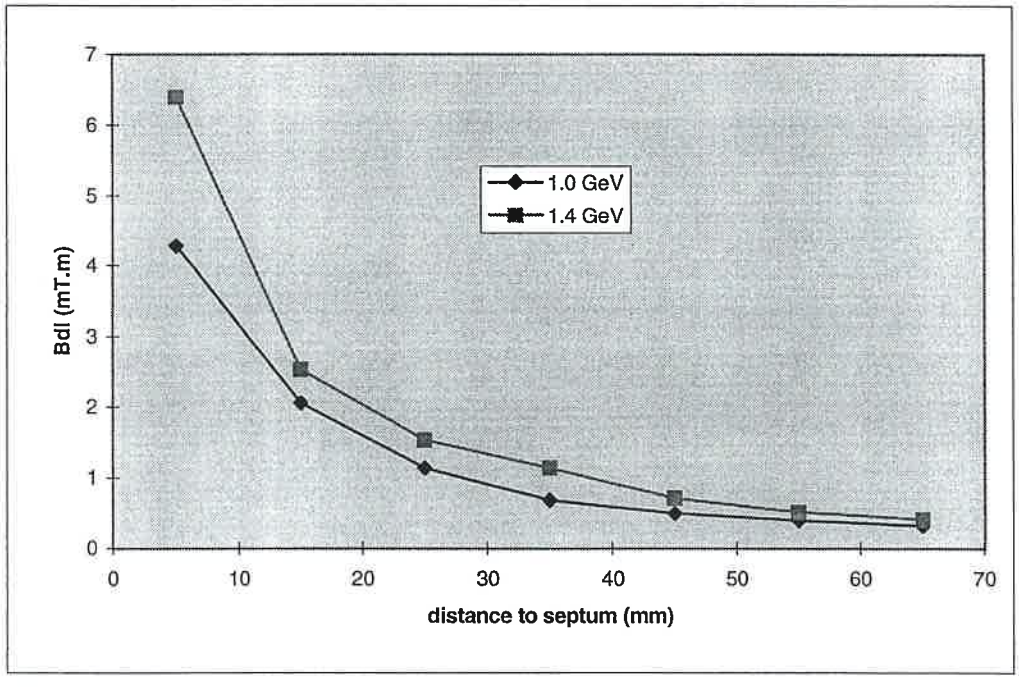

ENDFIELD smv20.1

date test: 12/12/96
coil 1 dia. 5 mm; 0.037 m2

distance to endplate (mm)	Vdt (V.s) 1.0 GeV, 20 kA	B (mT)	Vdt (V.s) 1.4 GeV, 25.16 kA	B (mT)
0	1.10E-03	29.78	1.38E-03	37.41
10	1.06E-03	28.59	1.32E-03	35.6
20	1.01E-03	27.30	1.28E-03	34.61
30	9.63E-03	26.08	1.22E-03	33.04
40	9.63E-04	25.42	1.17E-03	31.75
50	9.39E-04	24.41	1.14E-03	30.92
60	8.72E-04	23.62	1.09E-03	29.61
70	8.39E-04	22.73	1.06E-03	28.65
80	8.13E-04	22.00	1.02E-03	27.72
90	7.85E-04	21.27	9.83E-04	26.61
100	7.69E-04	20.82	9.65E-04	26.14
110	7.43E-04	20.10	9.28E-04	25.13

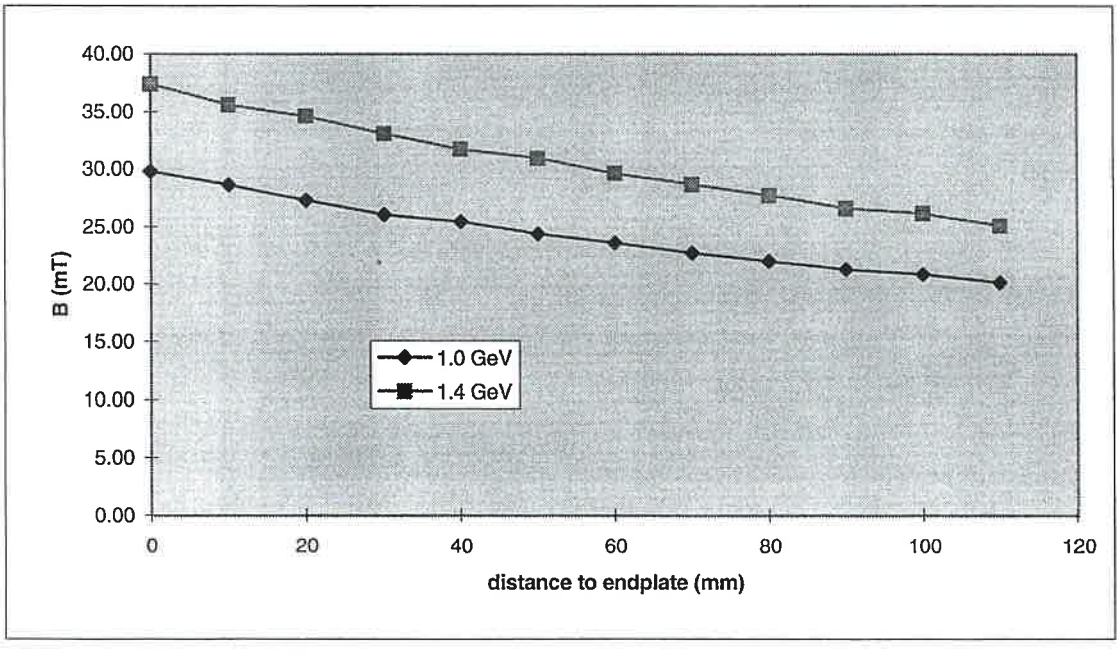

SMV20.2 - since ~ 2008

date test: 10/4/97

coil 1 dia. 5 mm; 0.03693 m2 (Bo)

coil 2 l=1300 mm 0.05769 m2/m (BdI) 0.0750 m2

I (A)	coil1 Vdt	mT	coil2 Vdt	mTm	Leq mm	remarks
17172	1.298E-02	351.6	2.019E-02	350.0	0.995	angle 73.2 mrad with protons at 0.8 GeV
18600	1.399E-02	378.9	2.179E-02	377.6	0.997	angle 79.3 mrad with protons at 0.8 GeV
19900	1.499E-02	406.0	2.331E-02	404.1	0.995	angle 73.2 mrad with protons at 1.0GeV
21560	1.630E-02	441.4	2.533E-02	439.1	0.995	angle 79.3 mrad with protons at 1.0GeV
25131	1.907E-02	516.5	2.967E-02	514.4	0.996	angle 73.2 mrad with protons at 1.4GeV
27226	2.068E-02	560.0	3.208E-02	556.1	0.993	angle 79.3 mrad with protons at 1.4GeV

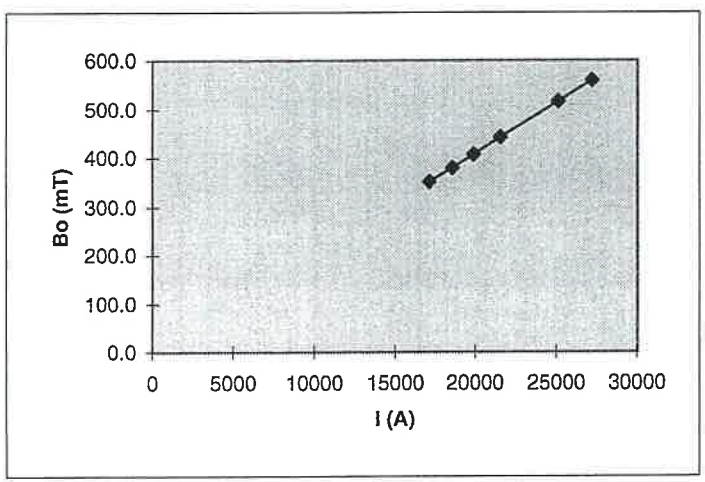

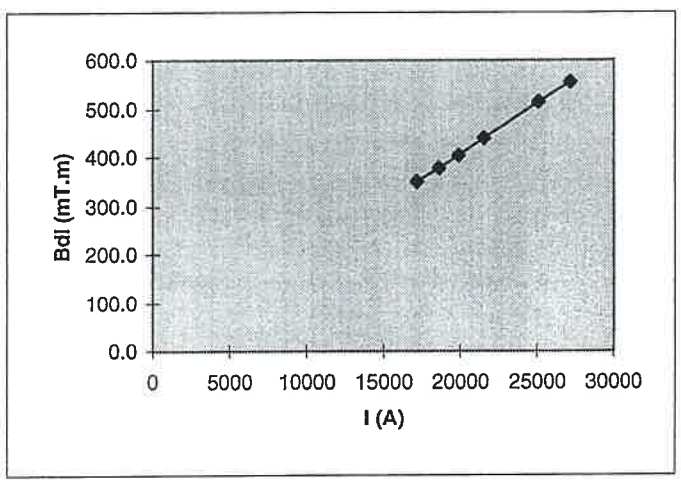

Fringefield SMV 20.2

date test: 10/4/96
coil 2 l=1300 mm 0.05769 m2/m
coil 3 l=1300 mm 0.05808 m2/m

distance to septum (mm)	Vdt (V.s) 1.0 GeV, 20 kA	Bdl (mT.m	Vdt (V.s) 1.4 GeV, 25.16 kA	Bdl (mT.m)		1/1000
5	2.52E-04	4.339	3.28E-04	5.646	coil3	10.97589
15	1.29E-04	2.137	1.60E-04	2.78	coil2	5.404355
25	7.34E-05	1.272	9.16E-05	1.588	coil2	3.087092
35	4.35E-05	0.746	5.77E-05	0.993	coil2	1.930404
45	3.13E-05	0.542	3.99E-05	0.6915	coil2	1.344285
55	2.27E-05	0.394	3.03E-05	0.5254	coil2	1.021384
65	1.90E-05	0.3298	2.50E-05	0.433	coil2	0.841757

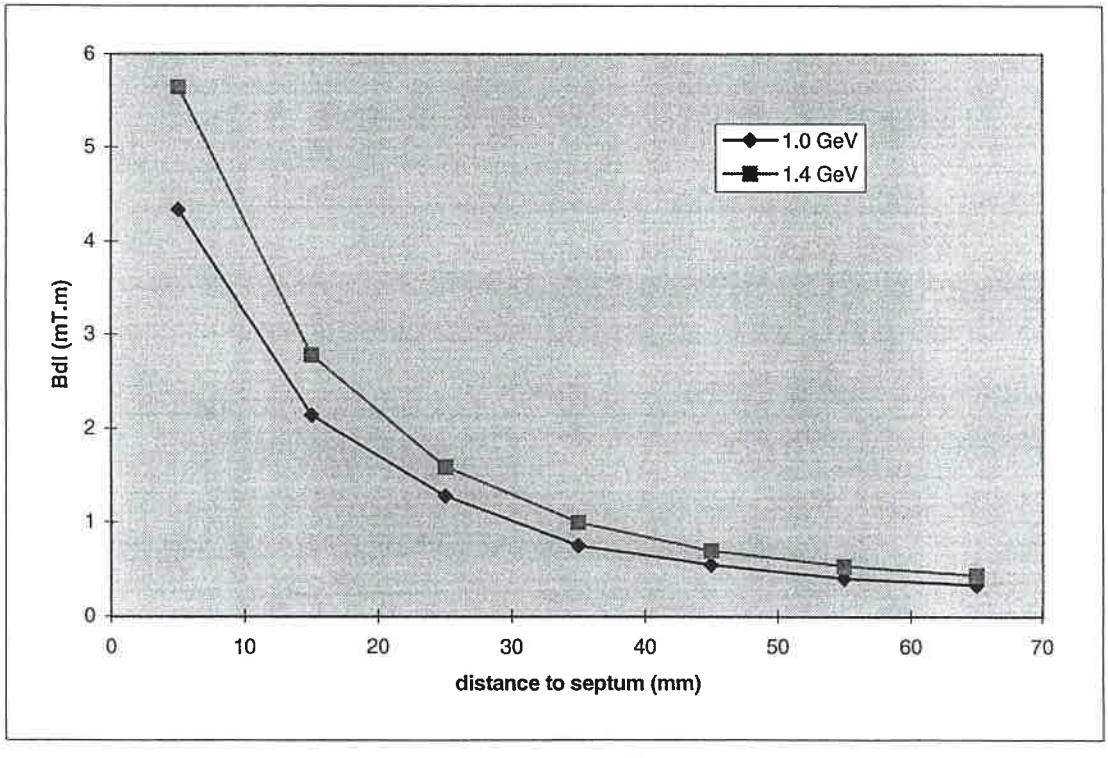

ENDFIELD smv20.2

date test: 10/4/97
coil 1 dia. 5 mm; 0.03693 m2

distance to endplate (mm)	Vdt (V.s) 1.0 GeV, 20 kA	B (mT)	Vdt (V.s) 1.4 GeV, 25.16 kA	B (mT)
0	5.60E-04	15.17	7.06E-04	19.12
10	2.71E-04	7.34	3.40E-04	9.2
20	1.52E-04	4.11	1.90E-04	5.156
30	9.19E-05	2.49	1.21E-04	3.288
40	6.20E-05	1.68	7.90E-05	2.138
50	4.21E-05	1.14	5.51E-05	1.49
60	3.06E-05	0.83	3.86E-05	1.044
70	2.19E-05	0.59	2.83E-05	0.7673
80	1.73E-05	0.47	2.22E-05	0.6016
90	1.27E-05	0.34	1.65E-05	0.4458
100	1.08E-05	0.29	1.33E-05	0.3609

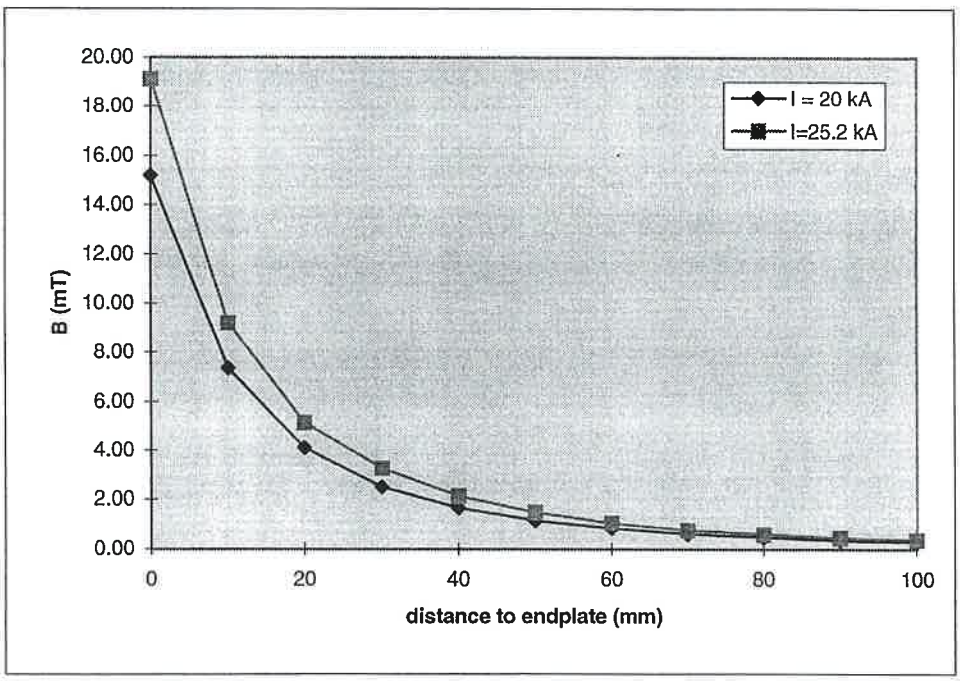

Appendix II: The preliminary septum magnet calculations

BT SMV 20 version pulsee

particularités

DONNEES		
particules electrons : e protons : p	p	
quant.mouvt : MV Energie cin. : EC	ec	
Energie cinétique Ec =	**0.8**	GeV
Déflexion requise	**73.2**	mrad
Epaisseur du septum	**5**	mm
Hauteur du Gap	**60.4**	mm
Profondeur du Gap	**116**	mm
Longueur magnetique equivalent	**1000**	mm
Espace de glissement	0	m
Monospire donc	**1**	spire
Epaisseur cond. retour	8.8	mm
Hauteur de conducteur retour	60.4	mm
Résistivité du cuivre (1.72E-2	0.0172	mO.mm
module d'Elasticité (12500	12500	daN/mm2
Forme de l'impulsion		
DC , 1/2 sinus : S , trapèze : T	S	
1/2 période de l'impulsion	**3.4**	ms
Période de récurence (cycle tot.	**1.2**	s
taux de répétition de l'impulsion de courant		
Systeme de refroidissement		
pression différentielle	**12**	bar
nombre du circuits	**2**	
septum		
forme element de refroidissement	**rec**	
Cote horizontal	**5**	mm
Cote vertical	**30.2**	mm
forme du passage d'eau	**circ**	
Diametre trou	**2**	mm
conducteur retour		
forme element de refroidissement	**rec**	
Cote horizontal (mm)	**8.8**	mm
Cote vertical (mm)	**30.2**	mm
forme du passage d'eau	**rec**	
Cote horizontal	**3.6**	mm
Cote vertical	**2.2**	mm
Matiere		
maximum admissible champ dans le f	**0.85**	T

RESULTATS	PROTONS	
Masse au repos mo	0.94	Gev/c2
Energie cinétique	**0.8000**	GeV
Quantité de mouvement	**1.4642**	Gev/c
beta	0.8415	
gamma	1.8511	
beta*gamma	1.5577	
Déplact. après espace de gliss	**36.6**	mm
Champ intégré B*L	**0.357**	T.m
Induction dans le Gap	**0.357**	T
Champ magn. H=B/uo	2.84E+05	A/m
Courant nécessaire	**17172**	A
Valeur efficace du courant	646	A
densité de courant eff.	**2.19**	A/mm2
Résistance de l'aimant	**0.104**	mOhms
Inductance de l'aimant	**2.27**	uH
Puissance dissipée	**0.043**	kW
Energie stockée	335	J

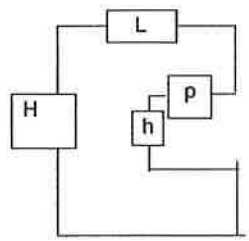

	116	p en mm
	60.4	h en mm
	164.8	L en mm
	157.9	H en mm
Débit d'eau total	**4.31**	l/min
Débit dans chaque spire	2.16	l/min
vitesse de l'eau dans septum	11.44	m/s
dT total d'eau	0.15	K
Force septum /cond fond	**306.76**	daN
Flèche max . septum (appui	0.007	mm
moment flech.max. (appui	2.32	mm*daN
contrainte maxi <5 (appui	0.56	daN/mm2
Masse culasse (sans poutre	**137**	**kg**
section cond. septum	295.7168147	mm2
Section refroidissement septur	6.283185307	mm2

M.THIVENT Version 12 Mai 1992 Edition du : 10.Dec.96

Modifie R, L pour monospire, hydraulique revise 2/8/94 J. Borburgh

PREDETERMINATION SEPTUM MAGNETIQUE SMCALC.XLS **PW prot:jb**

BT SMV 20 version pulsee

particularités

DONNEES		
particules electrons : e protons : p	**p**	
quant.mouvt : MV Energie cin. : EC	**ec**	
Energie cinétique Ec =	**1**	GeV
Déflexion requise	**73.2**	mrad
Epaisseur du septum	**5**	mm
Hauteur du Gap	**60.4**	mm
Profondeur du Gap	**116**	mm
Longueur magnetique equivalent	**1000**	mm
Espace de glissement	0	m
Monospire donc	**1**	spire
Epaisseur cond. retour	8.8	mm
Hauteur de conducteur retour	60.4	mm
Résistivité du cuivre (1.72E-2	0.0172	mO.mm
module d'Elasticité (12500	12500	daN/mm2
Forme de l'impulsion		
DC , 1/2 sinus : S , trapèze : T	**S**	
1/2 période de l'impulsion	**3.4**	ms
Période de récurence (cycle tot.	**1.2**	s
taux de répétition de l'impulsion de courant		
Systeme de refroidissement		
pression différentielle	**12**	bar
nombre du circuits	**2**	
septum		
forme element de refroidissement	**rec**	
Cote horizontal	**5**	mm
Cote vertical	**30.2**	mm
forme du passage d'eau	**circ**	
Diametre trou	**2**	mm
conducteur retour		
forme element de refroidissement	**rec**	
Cote horizontal (mm)	**8.8**	mm
Cote vertical (mm)	**30.2**	mm
forme du passage d'eau	**rec**	
Cote horizontal	**3.6**	mm
Cote vertical	**2.2**	mm
Matiere		
maximum admissible champ dans le f	**0.85**	T

RESULTATS	PROTONS	
Masse au repos mo	0.94	Gev/c2
Energie cinétique	**1.0000**	GeV
Quantité de mouvement	**1.6971**	Gev/c
beta	0.8748	
gamma	2.0638	
beta*gamma	1.8054	
Déplact. après espace de gliss	**36.6**	mm
Champ intégré B*L	**0.414**	T.m
Induction dans le Gap	**0.414**	T
Champ magn. H=B/uo	3.30E+05	A/m
Courant nécessaire	**19903**	A
Valeur efficace du courant	749	A
densité de courant eff.	**2.53**	A/mm2
Résistance de l'aimant	**0.104**	mOhms
Inductance de l'aimant	**2.27**	uH
Puissance dissipée	**0.058**	kW
Energie stockée	449	J

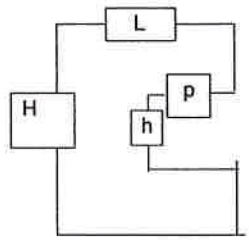

	116	p en mm
	60.4	h en mm
	172.5	L en mm
	173.4	H en mm
Débit d'eau total	**4.31**	l/min
Débit dans chaque spire	2.16	l/min
vitesse de l'eau dans septum	11.44	m/s
dT total d'eau	0.21	K
Force septum /cond fond	**412.07**	daN
Flèche max . septum (appui	0.009	mm
moment flech.max. (appui	3.11	mm*daN
contrainte maxi <5 (appui	0.75	daN/mm2
Masse culasse (sans poutre	**164**	**kg**
section cond. septum	295.7168147	mm2
Section refroidissement septur	6.283185307	mm2

M.THIVENT Version 12 Mai 1992 — Edition du : 10.Dec.96

Modifie R, L pour monospire, hydraulique revise 2/8/94 J. Borburgh

PREDETERMINATION SEPTUM MAGNETIQUE — SMCALC.XLS — **PW prot:jb**

BT SMV 20 version pulsee

particularités

DONNEES		
particules electrons : e protons : p	**p**	
quant.mouvt : MV Energie cin. : EC	**ec**	
Energie cinétique Ec =	**1.4**	GeV
Déflexion requise	**73.2**	mrad
Epaisseur du septum	**5**	mm
Hauteur du Gap	**60.4**	mm
Profondeur du Gap	**116**	mm
Longueur magnetique equivalent	**1000**	mm
Espace de glissement	0	m
Monospire donc	**1**	spire
Epaisseur cond. retour	8.8	mm
Hauteur de conducteur retour	60.4	mm
Résistivité du cuivre (1.72E-2	0.0172	mO.mm
module d'Elasticité (12500	12500	daN/mm2
Forme de l'impulsion		
DC , 1/2 sinus : S , trapèze : T	**S**	
1/2 période de l'impulsion	**3.4**	ms
Période de récurence (cycle tot.	**1.2**	s
taux de répétition de l'impulsion de courant		
Systeme de refroidissement		
pression différentielle	**12**	bar
nombre du circuits	**2**	
septum		
forme element de refroidissement	**rec**	
Cote horizontal	**5**	mm
Cote vertical	**30.2**	mm
forme du passage d'eau	**circ**	
Diametre trou	**2**	mm
conducteur retour		
forme element de refroidissement	**rec**	
Cote horizontal (mm)	**8.8**	mm
Cote vertical (mm)	**30.2**	mm
forme du passage d'eau	**rec**	
Cote horizontal	**3.6**	mm
Cote vertical	**2.2**	mm
Matiere		
maximum admissible champ dans le f	**0.85**	T

RESULTATS	PROTONS	
Masse au repos mo	0.94	Gev/c2
Energie cinétique	**1.4000**	GeV
Quantité de mouvement	**2.1429**	Gev/c
beta	0.9158	
gamma	2.4894	
beta*gamma	2.2797	
Déplact. après espace de gliss	**36.6**	mm
Champ intégré B*L	**0.523**	T.m
Induction dans le Gap	**0.523**	T
Champ magn. H=B/uo	4.16E+05	A/m
Courant nécessaire	**25131**	A
Valeur efficace du courant	946	A
densité de courant eff.	**3.20**	A/mm2
Résistance de l'aimant	**0.104**	mOhms
Inductance de l'aimant	**2.27**	uH
Puissance dissipée	**0.093**	kW
Energie stockée	716	J

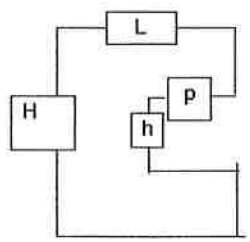

	116	p en mm
	60.4	h en mm
	187.4	L en mm
	203.1	H en mm
Débit d'eau total	**4.31**	l/min
Débit dans chaque spire	2.16	l/min
vitesse de l'eau dans septum	11.44	m/s
dT total d'eau	0.33	K
Force septum /cond fond	**657.02**	daN
Flèche max . septum (appui	0.014	mm
moment flech.max. (appui	4.96	mm*daN
contrainte maxi <5 (appui	1.19	daN/mm2
Masse culasse (sans poutre	**223**	**kg**
section cond. septum	295.7168147	mm2
Section refroidissement septur	6.283185307	mm2

Distribution:
M. Chanel
M. Martini
J.P. Riunaud
H. Schönauer
Section PS/CA/ Septa